Sex-specific recombination landscape in a species with holocentric chromosomes

Sebastian Chmielewski[1,5], Mateusz Konczal[1], Jonathan M. Parrett[1], Stephane Rombauts[2,3], Katarzyna Dudek[4], Jacek Radwan[1], Wiesław Babik[4]

[1] Evolutionary Biology Group, Adam Mickiewicz University, ul. Uniwersytetu Poznańskiego 6, 61-614 Poznań, Poland
[2] Department of Plant Biotechnology and Bioinformatics, Ghent University, 9052 Ghent, Belgium
[3] Center for Plant Systems Biology, VIB, 9052 Ghent, Belgium
[4] Institute of Environmental Sciences, Faculty of Biology, Jagiellonian University, Gronostajowa 7, 30-387 Kraków, Poland
[5] Corresponding author: Sebastian Chmielewski, Evolutionary Biology Group, Adam Mickiewicz University, ul. Uniwersytetu Poznańskiego 6, 61-614 Poznań, Poland. Email: schmielewski@amu.edu.pl

Abstract

The rate and chromosomal positioning of meiotic recombination significantly affects the distribution of the genetic diversity in eukaryotic genomes. Many studies have revealed sex-specific recombination patterns, with male recombination typically biased toward chromosome ends, while female recombination is more evenly distributed along chromosomes, or concentrated near the chromosome center. It has been proposed that such pattern in females may counteract meiotic drive caused by selfish genetic elements near centromeres and should not occur in species devoid of clearly defined centromeres, but evidence for the latter is scarce. Here, we constructed a sex-specific genetic map of a species with holocentric chromosomes, the bulb mite (*Rhizoglyphus robini*), a sexual selection model with alternative male reproductive phenotypes. We found a similar recombination landscape in both males and females, with a consistent pattern of increased rates towards both chromosome ends, and higher recombination rate in females than in males. A region on chromosome 7, carrying a high density of markers associated with the expression of alternative male reproductive phenotypes, was among several regions with particularly low male recombination rate. We detected a positive correlation between the recombination rate and the repeat density (highest at chromosome ends), and negative correlation with the gene density (peaking at chromosome centers). Our results are consistent with the meiotic drive hypothesis and suggest that recombination evolution is closely linked to the chromosome features.

keywords: recombination landscape, heterochiasmy, holocentric chromosomes, linkage mapping, genome anchoring

Introduction

Intragenomic heterogeneity of recombination rate is a major determinant of genetic variance through its effect on the efficacy of both positive and purifying selection (Coop & Przeworski, 2007; Ellegren & Galtier, 2016; Webster & Hurst, 2012). Therefore, interpretation of studies aiming to understand processes shaping genetic variation, a key parameter determining the response to selection, is likely to be incomplete unless one takes the genome-wide recombination landscape into account. Local recombination rates are influenced by several factors. They correlate with genomic features including the densities of genes and repeat elements, the GC content, and the distance to the chromosome end (reviewed in Peñalba & Wolf, 2020; Ritz et al., 2017; Stapley et al., 2017). Chromosomal rearrangements, including inversions (Berdan et al., 2021; Wellenreuther & Bernatchez, 2018), or

fusions and fissions (Näsvall et al., 2023), may also affect recombination rates. Moreover, large sex differences in recombination rates have been observed in many eukaryotic species (Lenormand & Dutheil, 2005; Stapley et al., 2017) with profound implications for the evolution of sex chromosomes (Charlesworth, 2017), the genetic architecture of complex sexually selected traits (Kasimatis et al., 2021), and the resolution of sexual conflict (Connallon & Clark, 2010).

Recent meta-analyses across a wide array of species have consistently highlighted sex differences in recombination rates, termed heterochiasmy, and in the distribution of crossover events along chromosomes, referred to as recombination landscape (Cooney et al., 2021; Lenormand & Dutheil, 2005; Sardell & Kirkpatrick, 2020). Female genetic maps are often longer than male maps, indicating a higher overall recombination rate in females. Heterochiasmy has been associated with various factors including differences in the intensity of sexual selection (Lenormand, 2003; Trivers, 1988), sexual antagonism (Sardell & Kirkpatrick, 2020), and the mechanistic differences during the progression of meiosis between males and females (Hunt & Hassold, 2002). The causes underlying sex-specific recombination landscapes are less well understood, though some mechanisms have been proposed (Cahoon et al., 2023; Sardell & Kirkpatrick, 2020). In females, crossovers are typically distributed evenly along the chromosomes or are somewhat biased towards chromosome centers. In contrast, males tend to exhibit recombination events near chromosome ends (Cooney et al., 2021; Peterson & Payseur, 2021; Sardell & Kirkpatrick, 2020).

The positioning of crossover events during meiosis is crucial from an evolutionary perspective because it regulates the amount of DNA exchanged between homologous chromosomes (Veller et al., 2019). If crossovers are strongly localized near chromosome ends in both sexes, the exchange of DNA occurs only at the chromosome tips, thereby largely preserving existing allelic combinations. Conversely, recombination near the centromere has been associated with a higher risk of chromosomal mis-segregation (Nambiar & Smith, 2016). This suggests that the pattern of crossovers in chromosome central regions has some benefits in female meiosis that outweigh this cost. One such benefit could be a defense against selfish elements causing meiotic drive. Unlike spermatogenesis, in which four gametes are produced, oogenesis results in a single viable egg and three inviable polar bodies. The segregation of chromosomes into the egg or a polar body is influenced by the centromere's efficiency in kinetochore binding (Clark & Akera, 2021; Talbert, Bayes, et al., 2009). Selfish genetic elements can exploit this mechanism by enhancing the centromere's size or activity, thus favoring their transmission to the egg rather than to polar bodies (Haig, 2010). Brandvain & Coop (2012) hypothesized that recombination near chromosome centers in females could represent an adaptive response to meiotic drivers, effectively uncoupling drive alleles from the centromere.

Organisms with holocentric chromosomes, which lack a localized centromere, could help to evaluate the meiotic drive hypothesis and the centromere's influence on the evolution of sex-specific recombination landscapes. According to the meiotic drive hypothesis, holocentric organisms are expected to have similar recombination landscapes in both sexes (Brandvain & Coop, 2012). This is because, in the absence of a localized centromere, allowing crossovers to occur nearer to the chromosome center in females would not confer any evolutionary advantage. Currently, research on recombination in holocentric chromosomes remains sparse, primarily limited to studies on *Caenorhabditis elegans* and Lepidoptera (moths and butterflies). However, *C. elegans* is hermaphroditic and appears to have a low recombination rate during spermatogenesis (Meneely et al., 2002), and Lepidoptera are not well suited for testing the meiotic drive hypothesis because meiosis is achiasmatic in females.

Holocentric chromosomes, characterized by a diffuse centromere, have been found in approximately 350,000 animal and plant species (Král et al., 2019). Among these, acariform mites represent a group

of particular interest due to their diverse roles in ecosystems and impacts on human activities. The acariform mites include species of economic importance such as agricultural pests (e.g., the spider mites *Tetranychus urticae* and bulb mites *Rhizoglyphus robini*) and allergenic species (e.g., dust mites *Dermatophagoides spp*.). However, genomic resources for mites remain scarce, and, to date, no sex-specific whole-genome linkage map has been published for any mite species. Considering the over 40 thousand described acariform species (Walter & Proctor, 2013), only five species currently have genomes assembled to chromosome-scale resolution. Next-generation sequencing technologies hold promise for the development of detailed genetic maps, which can be used for anchoring genomes to a chromosome scale (Fierst, 2015), and should yield reliable data concerning recombination patterns and possible sex differences (Peñalba & Wolf, 2020).

Here, we developed sex-specific linkage maps of the bulb mite (*Rhizoglyphus robini*), and characterized the genomic factors that often correlate with local recombination rates. Furthermore, we used the linkage map to obtain a chromosome-scale genome assembly. Bulb mites are economically important pests (Díaz et al., 2002), but also a convenient laboratory model (Gerson et al., 1991) used in evolutionary and ecological studies (e.g. Plesnar-Bielak et al., 2013; Smallegange et al., 2017). In particular, it is valuable for studies of sexual selection, due to the presence of two distinct male morphs differing in expression of a sexually selected trait (Radwan, 2007). Fighter males possess an enlarged third pair of legs which they use as a weapon in intrasexual competition, while scrambler males, with unmodified legs, adopt a non-aggressive strategy to obtain access to females (Radwan, 2009). A recombination map anchored to the genome assembly will facilitate identification of genomic regions affecting male morph determination, a trait which shows high additive genetic variance (Parrett et al., 2023). Pinpointing these regions has been problematic due to highly fragmented bulb mite genome assembly that has been published recently (Parrett et al., 2022). Finally, our linkage map allows us to examine the heterochiasmy and sex-specific recombination patterns in a species with holocentric chromosomes. This has implications for the meiotic drive hypothesis proposed by Brandvain & Coop (2012), which has not yet received empirical support.

Materials and methods

Experimental crosses

We used inbred lines established by 10 generations of sib-crossing before the experiment started (Łukasiewicz et al., 2020; Parrett et al., 2023). Four mapping families were created by crossing mites from different lines. Mites were housed at 23°C in glass vials (~1 cm diameter) with a plaster-of-Paris base soaked in water to maintain high humidity and fed with dry yeast ad libitum.

To select individuals for the crosses, we isolated juvenile mites from the inbred lines into separate glass vials, to ensure the females eclosed were virgins. Upon reaching maturity, we scored the mites for sex and male morph, then paired a single male and female in new vials to form the parental P-generation. After three days of mating, P individuals were transferred to low-DNA-binding tubes containing DNA isolation buffer (digestion solution from the MagJET gDNA Kit, Thermo Fisher Scientific) and stored at -20°C for subsequent DNA extraction. The eggs were left to hatch in the vials. The emerged F1 mites were separated into individual vials before reaching maturity, and subsequently sexed and mated with full-sibs. For each of the four families, we selected the F1 pair with the highest reproductive output for further breeding (Table 1). We separated F2 individuals as larvae, sexed them when mature, and then placed them in the DNA isolation buffer. In total, we used 199 bulb mites from the four families to construct the genetic map, comprising 8 P, 8 F1, and 183 F2 individuals, with the number of F2 individuals per family ranging from 32 to 60 (Table 1).

136 ***Repeat masking***

137 We identified repeat sequences in the VIB_bulbmite_20200 genome assembly (Parrett et al., 2022)
138 using the RepeatModeler pipeline, which integrates several software tools each designed to detect
139 specific types of repeats (Flynn et al., 2020). This process produces a FASTA library of representative
140 repeat elements, which was annotated to classify the types of repeats found. We then combined this
141 file with the Repbase public reference data files, which contain known repeat elements from other
142 organisms, to enhance the completeness of our library (Jurka et al., 2005). We used the merged FASTA
143 library with RepeatMasker (http://www.repeatmasker.org, Tarailo-Graovac & Chen, 2009) to mask the
144 genome before proceeding with mapping and annotation. The repeats were soft-masked (bases in
145 masked regions were indicated by lowercase letters).

146 ***Whole-genome resequencing and calculating genotype likelihoods***

147 We extracted genomic DNA from whole individuals using the MagJet Genomic DNA Isolation Kit
148 (Thermo Fisher Scientific), following the kit's standard protocol. Next, we prepared genomic libraries
149 with the NEBNext Ultra FS II kit (New England Biolabs) and resequenced the whole genomes at the
150 SNP&SEQ Technology Platform in Uppsala, Sweden using Illumina NovaSeq6000 with the S4 flow cell,
151 producing paired-end reads of 150 bp in length. We aimed for an expected coverage of 20X for parental
152 and F1 samples, and 10X for the F2 samples.

153 To clean the data, adapter sequences and low-quality bases were removed using Trimmomatic (v.
154 0.39; Bolger et al., 2014). The reads were mapped to the VIB_bulbmite_20200 genome assembly
155 (Parrett et al., 2022) using bwa-mem (v. 0.7.17; Li, 2013) with default settings. Samtools (v. 1.19; Li et
156 al., 2009) was used to mark duplicates and retain only reads with mapping quality above 20.

157 To address genotyping errors arising from low sequencing coverage, instead of calling genotypes, we
158 calculated genotype likelihoods for the initial set of SNPs using samtools mpileup and the
159 mpileup2Likelihoods script (Rastas, 2017). We assessed the relatedness between individuals within
160 each family using the Identity By Descent (IBD) module of Lep-Map3 (Rastas, 2017), using a subset of
161 random 10% of the markers.

162 ***Linkage mapping***

163 We constructed the bulb mite genetic map using Lep-Map3, following its standard pipeline. Initially,
164 the ParentCall2 module was used to correct missing or erroneous parental genotypes, eliminate non-
165 informative markers, and identify sex-linked markers. We filtered out markers showing significant
166 segregation distortion (dataTol = 0.05), those with a minor allele frequency across families below 0.15,
167 and those with a missing genotype rate within families exceeding 10%. Two F2 samples were discarded
168 due to insufficient sequencing coverage (<0.1X), and one was excluded due to its high rate of missing
169 data, as determined by PLINK (v. 1.9; see supplementary data). We retained only markers that were
170 informative across all four families, except when a contig had fewer than five markers; in such cases,
171 we included markers informative in three families. To assign markers to linkage groups,
172 SeparateChromosomes2 was used with a LOD threshold optimized by testing values from 15 to 19. We
173 chose the threshold that distributed markers into eight linkage groups, the bulb mite haploid
174 chromosome number (Parrett et al., 2022)

175 We generated a sex-averaged map using OrderMarkers2 with the Kosambi mapping function, relying
176 on P-generation data to phase the F1 and F2 genotypes. The bulb mite has an XX/X0 sex-determining
177 system. In contrast to the diploid autosomes, males carry only a single copy of the X chromosome.
178 Therefore, only female-informative markers were used to establish the marker order on the sex

chromosome. The ordering was repeated 60 times, selecting the iteration with the highest likelihood for our final map. Single markers that extended the ends of the chromosome map by more than 1 cM were excluded, as these are likely to indicate genotyping errors. LMPlots visualized with Lep-Map3 highlighted a single error on chromosome 4, which we corrected by removing three adjacent crossovers, following the software author's recommendation (Pasi Rastas, personal communication; see supplementary data and Figure S6).

Genome anchoring

Lep-Anchor (Rastas, 2020) was used to anchor the bulb mite genome, based on the intervals of genetic marker positions determined by OrderMarkers2. The anchoring process was supported by Oxford Nanopore reads, which had also been used for assembling the original reference genome (Parrett et al., 2022), and were mapped to the reference genome with minimap2 (v. 2.24; Li, 2018).

To identify haplotigs—false apparently duplicated regions arising from high local heterozygosity—we used HaploMerger2 (Huang et al., 2017) with a custom score matrix and a chain file containing contig-contig alignments. Genetic markers from the haplotigs were transferred to the primary contigs using the LiftoverHaplotype module. Additionally, we identified a chimeric contig that erroneously spanned two chromosomes, which we split using CleanMap. PlaceAndOrientContigs was used to determine the order and orientation of contigs on chromosomes. This module organizes the contigs by iteratively maximizing the correlation between the physical and genetic distances of markers. Subsequently, the contigs were propagated using the long ONT reads and the chain file. Contig blocks without map support were removed. In the final step, we adjusted the chromosome labels to reflect their physical sizes.

Evaluation of the linkage map

We evaluated the genetic map based on the physical positions of markers after anchoring. The evaluation was conducted using the OrderMarkers2 module with the Kosambi mapping function, applying parameters: UsePhysical, ImproveOrder = 0, and EvaluateOrder = 1, using P-generation data to phase genotypes. To produce sex-specific maps, we generated a female map using markers informative in mothers or in both parents (infMask = 23), and a male map with markers informative in fathers or in both parents (infMask = 13). The evaluation of the sex chromosome was based only on the female-informative markers (infMask = 2). Diagnostics of the map using LMPlot identified a mis-join on chromosome 6, which we resolved by removing three adjacent crossovers, following guidance from Pasi Rastas (personal communication, see supplementary data and Figure S7). We analyzed the maps with custom R scripts and visualized them using the ggplot2 R package (Wickham, 2016).

Recombination landscape and heterochiasmy

We investigated the relationship between chromosome length and recombination rate or map length using linear models (LMs), incorporating sex as a categorical variable to allow for possible differences between males and females. To explore the sex-specific recombination landscape, we calculated recombination rates in 1Mb non-overlapping genomic windows by dividing the total genetic length of windows by their physical lengths. To standardize the comparison of the recombination landscape across all chromosomes, we scaled their lengths to unity by dividing the window positions by the total length of the relevant chromosomes. The recombination landscape was visualized separately for the male and female maps along each chromosome using a LOESS smoothing line, with a span parameter of 0.75. Notably, we observed a sharp increase in recombination rate near chromosome ends. To quantify this effect, we calculated a periphery bias by dividing the recombination rate in the outer 10%

of the physical length at each chromosome end (distal parts) by the average recombination rate across the entire chromosome, following Haenel et al. (2018).

To investigate whether sex differences in crossover positioning contribute to the variation in the amount of DNA exchanged during meiosis, we calculated the probability that a random pair of positions (also referred to as a "locus") from the same chromosome will recombine due to a crossover event (termed *intrachromosomal shuffling*, or $\overline{r}_{intra}$ by Veller et al., 2019), using the following equation:

$$\overline{r}_{intra} = \sum_{k=1}^{n} 2p_k r_k L_k^2$$

In this equation p_k denotes the proportion of chromosome k carrying one parental haplotype, while r_k represents the proportion of the same chromosome inherited from the other parent. L is the proportion of the entire genome contributed by chromosome k. Due to minor gaps in phasing, as shown in Figure S9, the sum of, $p_k + p_l$ does not equal 1 (see Figure 5 in Veller et al., 2019). Next, we estimated the probability of recombination between two loci located on different chromosomes (interchromosomal shuffling, or $\overline{r}_{inter}$) using the following equation:

$$\overline{r}_{inter} = \frac{1}{2}\left(1 - \sum_{k=1}^{n} L_k^2\right)$$

Identification of genomic features affecting recombination rate

To assess which features within the bulb mite genome correlate with the recombination rate, we explored the relationship between crossover counts in 2 Mb windows and the following genomic features: gene and repeat element density, distance to chromosome ends, and GC content. We downloaded the bulb mite genome's predicted gene annotation from ORCAE (Parrett et al., 2022; Sterck et al., 2012), https://bioinformatics.psb.ugent.be/gdb/Rhizoglyphus_robini), which contains an unexpectedly high number of predicted genes (60,310 genes), suggesting the presence of pseudogenes or gene prediction errors. To refine the dataset, we excluded genes with expression levels below 1 FPKM, based on expression data from Plesnar-Bielak et al. (2022). This filtering retained 27,363 genes mapped to chromosomes. We determined the proportion of each window covered by genes (including introns), splitting genes at window boundaries when necessary. Repetitive sequences were quantified from the de novo dataset described above, and the distance to chromosome ends was calculated from each window's midpoint. The GC content of windows was determined using bedtools nuc (v2.27.1,Quinlan & Hall, 2010). Given the substantial collinearity among genomic features and the absence of crossovers in many windows, directly modeling associations with recombination counts proved challenging. Instead, we calculated Pearson's correlation coefficients (ρ) between crossover count and genomic features in 50 kb windows.

Results

Sequencing and linkage mapping

Whole-genome resequencing of the 196 samples in our families yielded a total of 6.26×10^9 reads. After mapping and removal of reads with low mapping quality, we retained 4.43×10^9 reads and 196 individuals (Table S1). The mean coverage was 21.3X in the P and F1 samples, and 9.25X in the F2 samples. Filtering based on minor allele frequency, family informativeness, and segregation distortion

reduced the number of SNPs from 8,709,873 to 332,682. Subsequently, 300,355 markers (90.3% of the filtered SNPs) were assigned to 8 linkage groups, which were used to construct the linkage map.

Linkage map

The bulb mite autosomal map included 254,226 markers. The female autosomal map spanned 257.81 cM, being 2.08 times longer than the male autosomal map (123.98 cM; Figure 1A). The high density of markers allowed us to obtain high resolution, with a mean inter-marker distance of 881 bp in the female map and 921 bp in the male map. The sex chromosome, which is hemizygous in males, comprised 45.5 thousand markers across 51.6 cM and showed the highest recombination rate among all chromosomes in both sexes**,** at 1.74 cM/Mb. Our analysis revealed a negative association between chromosome size and the mean recombination rate (LM: recombination rate ~ physical length + sex, adjusted R^2 = 0.68, *P* for the physical length = 0.035, Figure 1B). However, this observed pattern was primarily influenced by a particularly long chromosome 1, as the association becomes insignificant once chromosome 1 is excluded from the analysis (R^2 = 0.58*, P* = 0.39). However, the association between the physical and map lengths of autosomes was not significant (LM, adjusted R^2 = 0.63, *P* = 0.86, Figure 1C), and genetic lengths of male and female maps were not significantly associated either (LM, adjusted R^2 = -0.19, *P* = 0.82, Figure 1D).

Heterochiasmy, recombination landscape and allelic shuffling

Consistent with the genetic map length, the genome-wide autosomal recombination rate was 2.08 times higher in females than in males, with females exhibiting a mean recombination rate of 1.11 cM/Mb and males only 0.56 cM/Mb (Table 2). The sex-averaged recombination rate in bulb mites was 0.86 cM/Mb. In total, 516 crossovers were identified in female, and 205 in male parents.

The degree of heterochiasmy differed between chromosomes (Figure 1A, Table 2). Among chromosomes with markedly low recombination rate in the male map was chromosome 7, (Figure 1A), which harbors high density of SNPs associated with the male morph (Parrett et al., 2022, Chmielewski et al., unpublished data). A similarly low male recombination rate is observed on chromosome 1.

Analysis of the periphery bias and the recombination rates across all chromosomes revealed a similar recombination landscape in both males and females, with a consistent pattern of increased rates towards both chromosome ends (Figure 2A). Notably, the value of periphery bias exceeded 1 for all chromosomes (Table 2), indicating that recombination rates at chromosome ends were consistently higher than in their central regions. Periphery bias did not show significant association with either sex or with chromosome length (LM: periphery bias ~ sex + chromosome length; adjusted R^2 = 0.004, *P* = 0.39).

The estimated sex-averaged value of $\overline{r}_{intra}$ in the bulb mite genome was 0.43. However, we found that the $\overline{r}_{intra}$ was three times higher in females than in males ($\overline{r}_{intra\ females}$ = 0.0089, $\overline{r}_{intra\ males}$ = 0.0028, Figure 2B). This difference could be attributed to the variation in either crossover location, or the overall recombination rate, since a higher frequency of recombination in one sex could increase the value of $\overline{r}_{intra}$. Given the largely similar recombination landscape between sexes, underscored by the lack of significant sex-based differences in periphery bias, the observed difference in $\overline{r}_{intra}$ probably arises primarily from the increased recombination rate during female meiosis. $\overline{r}_{intra}$ values were not significantly associated with the chromosome lengths (LM: $\overline{r}_{intra}$ ~ sex + chromosome length; *P* = 0.16, adjusted R^2 = 0.14).

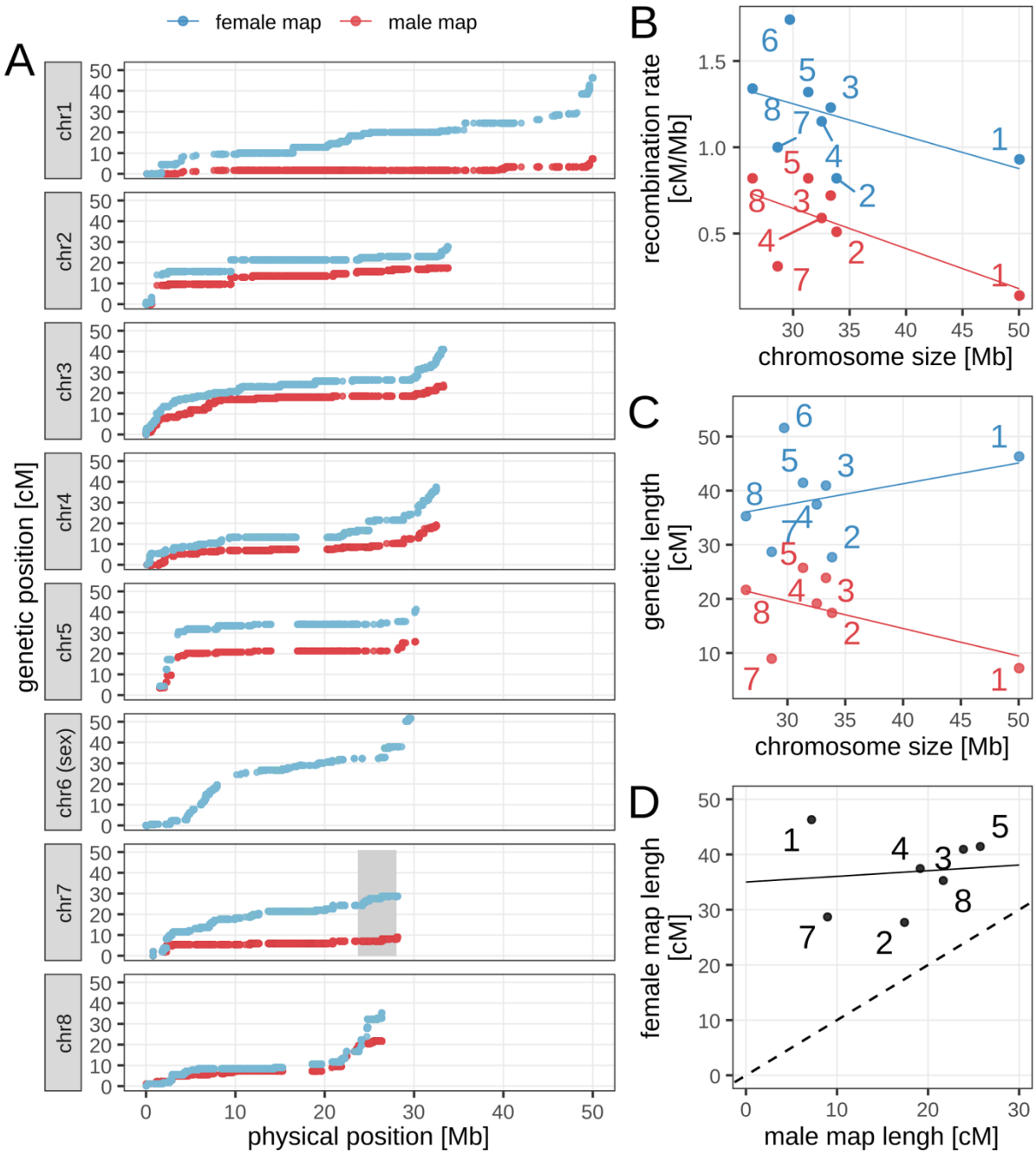

Figure 1: Sex-specific meiotic linkage maps and chromosome map length variation in the bulb mite. A: Marey maps displaying the genetic positions of markers in relation to their physical locations on the chromosomes. Regions with little change in genetic position, usually in chromosome centers, have low recombination rates, while steep slopes indicate high recombination rates. The locus responsible for determining male morph has been highlighted on chromosome 7. B: The relationship between recombination rate and chromosome size, showing higher recombination rates in shorter chromosomes ($P = 0.028$). C: The relationship between chromosomal map length and its physical size is not significant ($P = 0.86$). D: Comparison of map lengths for 7 autosomes, with female map lengths plotted against male map lengths. The dashed line indicates expected relationship under equal map lengths for both sexes, and the solid line the observed regression slope ($P = 0.82$).

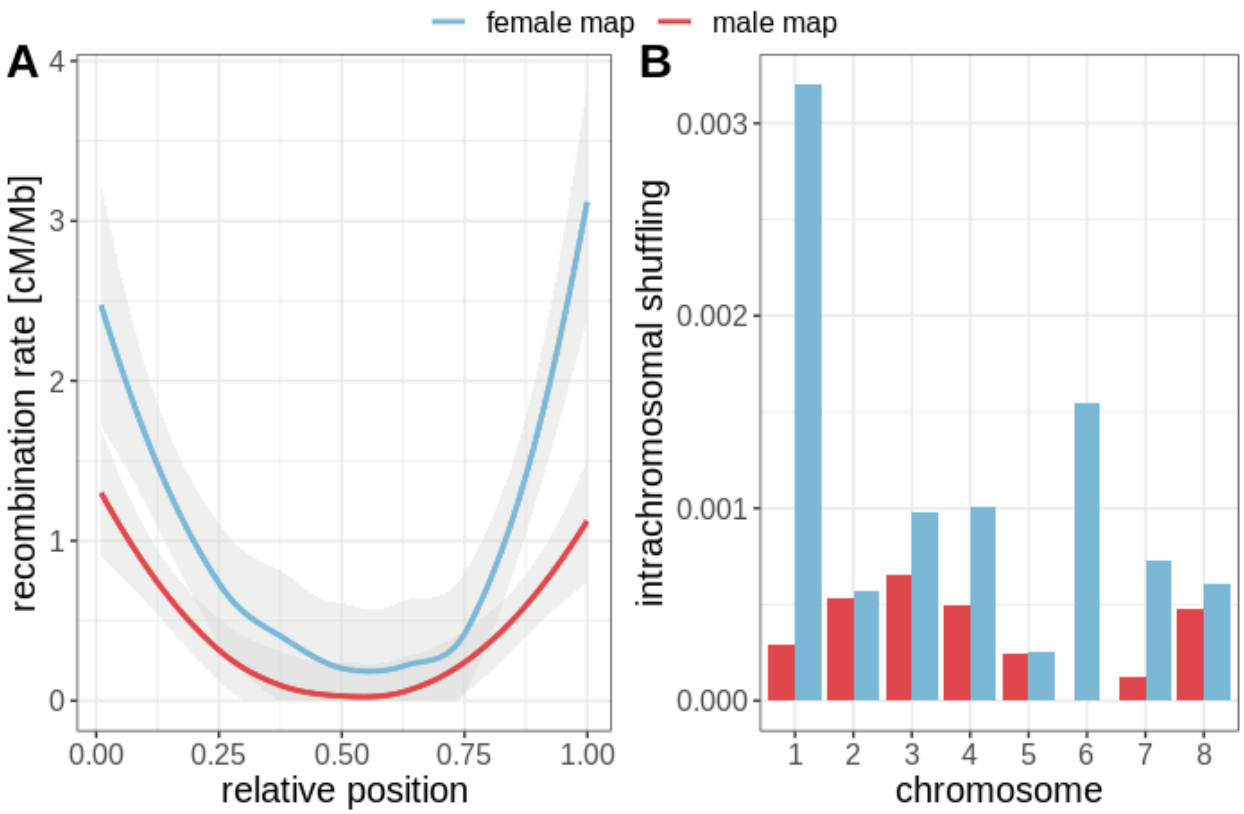

Figure 2 Sex-specific recombination patterns in the bulb mite genome. A: Smoothed loess line visualization of the recombination rates along the relative positions of all chromosomes, with the rates generally being lower in the central regions. The x-axis represents the relative position along the chromosomes, normalized from 0 to 1. B: The bar graph representing the average intrachromosomal shuffling value for each chromosome. Chromosome 6 is the sex chromosome.

Anchoring the bulb mite genome

The linkage map was used to anchor the contigs in order to obtain a chromosome-level genome assembly (Figure 1). A total of 397 contigs, accounting for 89.9% of the genome size, were successfully anchored onto 8 chromosomes. A total of 3.13 Mb, corresponding to 1.06% of the previous assembly length, was identified as redundant haplotigs and subsequently removed. Consequently, the overall genome size was reduced from the previous estimate of 307.49 Mb to 295.62 Mb, close to the 293 Mb predicted by flow cytometry (Parrett et al., 2022). The assembly's N50 value improved from 1.59 Mb for the previous bulb mite reference genome, to 32.53 Mb. The BUSCO score corroborates the high quality of the assembly, with 93.60% of the 2,934 core arachnid genes detected as complete (86% identified as full-length single-copy and 7.6% as duplicated), 1.6% classified as fragmented and only 4.8% missing. High N50 and BUSCO scores, along with the significant integration of the genome sequence into chromosomes, imply a comprehensive chromosome-level assembly, complete enough for accurate genomic feature characterization and recombination landscape analysis in the bulb mite genome.

Aside from chromosome 1, the bulb mite chromosome sizes are quite uniform, ranging from 26-34 Mb. Overall, bulb mite chromosomes have gene-rich centers, with gene density tapering off towards the chromosome ends (Figure 3). The distribution of GC content mirrors that of gene density, while repeat density shows the inverse pattern, peaking near chromosome ends. Noteworthy, the sex

chromosome showed the greater abundance of repeat sequences (t-test = -2.65, $P = 0.008$) and lower gene density (t-test = - 25.17, $P < 0.001$) in 50 kb windows, compared to the autosomes.

Repeat sequences constitute 28.77% (85.06 Mb) of the bulb mite genome, with the most prevalent identified repeats being LTR retrotransposons and simple repeats, representing 2.07% and 1.98% of the genome length, respectively (Table 3). Notably, a significant proportion of repeats were unclassified. SINE transposons were absent in the assembly.

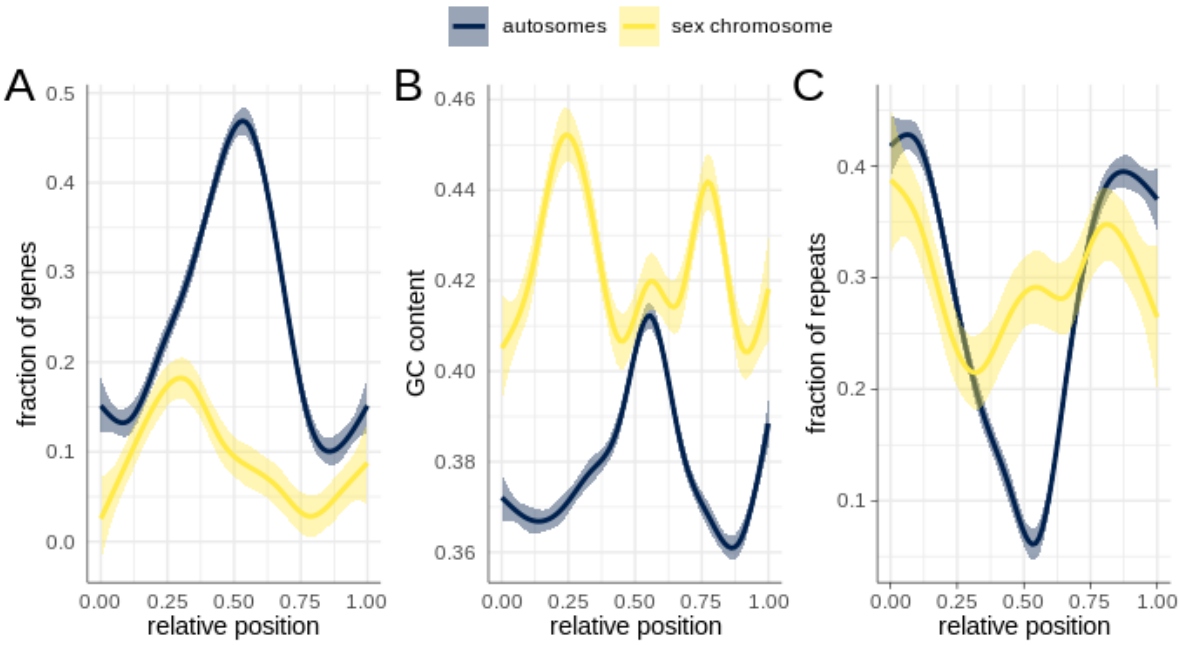

Figure 3 Distribution of the genetic features across the autosomes and the sex chromosome in the bulb mite genome. Three measures are plotted in non-overlapping 50 kb windows, whose midpoints are normalized by the chromosome's total length, to show the results for relative chromosomal positions, and smoothed by a loess line with a 95% standard error. A: The proportion of window length covered by genes (including introns), B: GC nucleotides, C: repetitive elements.

Genomic features correlated with local recombination rate

To investigate the genomic features correlated with the recombination rate across the genome, we computed Pearson's correlation coefficients in 2 Mb windows. The crossover count is negatively correlated with both gene density ($\rho = -0.27$, $P = 0.0013$; Figure 4) and distance to chromosome ends ($\rho = -0.41$, $P < 0.0001$). In contrast, it was positively correlated with repeat density ($\rho = 0.3$, $P = 0.0003$). No significant correlation was found between crossover count and GC content ($\rho = -0.16$, $P = 0.063$).

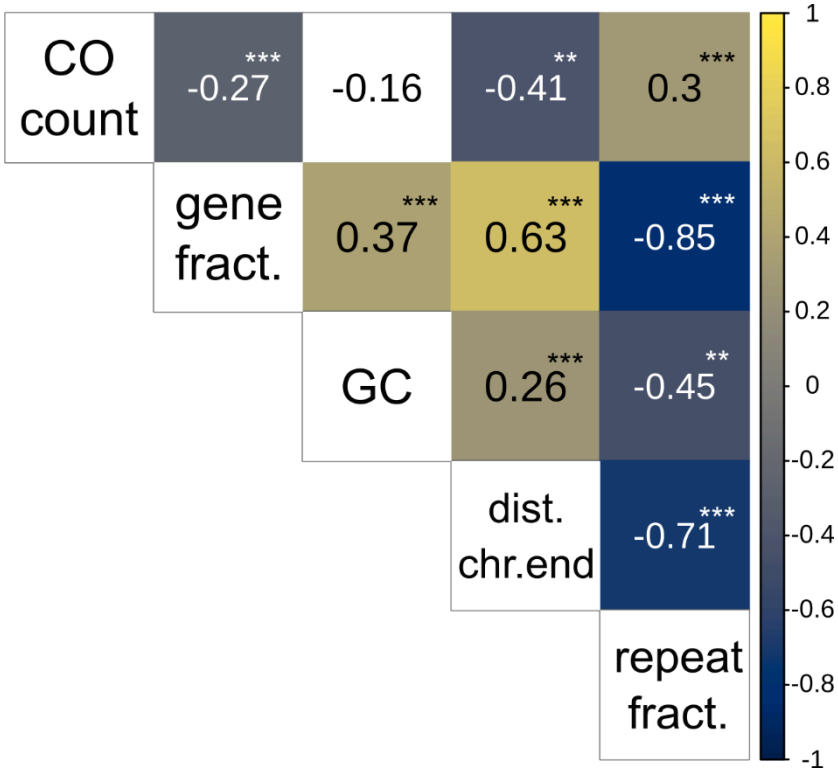

Figure 4: Correlation matrix showing Pearson's correlation coefficients. The matrix represents Pearson's correlation coefficients between various genomic features, with the intensity of the color indicating the strength and direction of the correlation (yellow for positive, blue for negative). Statistical significance levels are denoted by asterisks (*** *for* $P < 0.001$, ** for $P < 0.01$, and * for $P < 0.05$).

Discussion

To our knowledge, our genetic linkage map of *Rhizoglyphus robini* is the first sex-specific map for a gonochoristic organism with holocentric chromosomes. The absence of localized centromeres in chromosomes of this species enabled us to use our genetic map, constructed using whole genomes from nearly 200 individuals, to obtain a chromosome-level assembly of bulb mite, and then to evaluate the meiotic drive hypothesis. Our results demonstrated that the recombination landscapes for females and males are similar, supporting the role of meiotic drive in evolution of sex specific recombination landscapes.

Our assembly of bulb mite chromosomes also allowed us to characterize the distribution of genomic features along them. We found a unimodal gene distribution with a central peak, the opposite of the distribution of repetitive elements. This pattern, with elevated recombination rates at chromosomal ends, mirrors the genomic architecture seen in *C. elegans*, another species with holocentric chromosomes (The *C. elegans* Sequencing Consortium, 1998). By contrasting these observations with other species, we discuss the evolutionary importance of centromeres in the evolution of sex differences in recombination landscapes.

The bulb mite genome

The bulb mite genome, with a size of 295.62 Mb, is one of the largest acariform mite genomes. This group is characterized by notably compact genomes, with a median size of 129 Mb and a range from 32.5 to 487 Mb (Gregory & Young, 2020; Xiong et al., 2020). Our high-density linkage map enabled us to anchor 90% of the assembled genome length to chromosomes and to remove redundant haplotigs.

Anchoring revealed that the chromosome sizes are fairly constant (Table 2), apart from chromosome 1 which is almost twice longer than other chromosomes. Conceivably, increased size of this chromosome could be a result of chromosome fusion, which is further supported by its low recombination rate, characteristic of fused chromosomes (Näsvall et al., 2023), and bimodal distribution of gene, GC and repeat content of this chromosome (Figure S8).

Bulb mite chromosomes are characterized by gene-rich and GC-rich chromosome centers, as well as a high density of repetitive elements at the chromosome ends, similar to those observed in other holocentric animals (Cicconardi et al., 2021; The *C. elegans* Sequencing Consortium, 1998; Zhou et al., 2023). The sex chromosome exhibits a significantly lower gene density compared to autosomes, like in other holocentric organisms with X0 sex determination systems (Anderson et al., 2022; Y. Li et al., 2019; The *C. elegans* Sequencing Consortium, 1998). However, the pattern of reduced gene content on the sex chromosome is not universal and appears to depend on the age of the sex chromosome. Indeed, a similar gene density between autosomes and sex chromosomes has been reported in the dragonfly *Pantala flavescens* (Liu et al., 2022).

Repeated sequences constitute 28% of the bulb mite genome, nearly double the amount found in *Tyrophagus putrescentiae*, the only other acarid species with an available chromosome-scale reference genome assembly (Zhou et al., 2023). Importantly, most of these repeats have not been assigned to any known repeat category, indicating a potential area for future research. The observation that the sex chromosome is enriched in repeats compared to autosomes (Figure 3C), is probably because the sex chromosome spends one-third of its time in males in which it does not recombine; its overall recombination rate per generation is therefore lower than that of autosomes, The X chromosome also has a lower effective population size than the autosomes. At a 1:1 sex ratio, there are 4 autosomes per 3 X chromosomes, which might also contribute to the X chromosome having a higher expected repeat density, and lower gene density. These combined effects of reduced recombination rate and effective population size leads to higher Hill-Robertson interference, a genetic phenomenon where linked loci interfere with each other's ability to respond to natural selection. Consequently, TE insertions, which are generally harmful, are less effectively eliminated from the sex chromosome.

Genome-wide and chromosomal recombination rates

The sex-averaged recombination rate observed in the bulb mite is 0.86 cM/Mb, similar to the mean rate observed across insects (1.03 cM/Mb, Stapley et al., 2017; Wilfert et al., 2007). The closest relative of the bulb mite that has been genetically mapped, the spider mite *Tetranychus urticae*, exhibits a significantly higher recombination rate of 7.63 cM/Mb (Sugimoto et al., 2020). In contrast, the recombination rate of more distantly related deer tick, *Ixodes scapularis* (Ullmann et al., 2003), has been estimated at 0.006 cM/Mb. However, the estimate for the *I. scapularis* was based on only 127 markers for the genome size of 2.1 Gb, compared to almost 300 thousand markers used in our study. Consequently, this may lead to an underestimation of recombination rate, for instance, if terminal markers were not consistently included and many crossover events occurred in terminal regions.

In our study, we observed that longer chromosomes had lower recombination rates (Figure 1B). This may reflect the requirement for at least one crossover per chromosome in eukaryotes (Brazier & Glémin, 2022a; Hughes & Hawley, 2020; Otto & Payseur, 2019; Stapley et al., 2017), except in species in which meiosis in one sex is achiasmate (e.g., Lepidoptera females and Drosophila males), where alternative mechanisms have evolved to ensure proper chromosome segregation. Nevertheless, a chromosome's physical and map lengths were not associated (Figure 1C). This may be due to undetected recombination events, perhaps especially in male meiosis, as suggested by the relatively short genetic length of chromosomes (Table 2, Figure 1A). Given high density of marker distribution

and accurate phasing based on the grandparental generation (Figure S9), it is unlikely that we missed crossovers perhaps except for close proximity of chromosome ends, where informative markers were absent. In monocentric chromosomes, such terminal chiasmata can lead to improper chromosome segregation due to insufficient tension between homologues, resulting in premature sister chromatid separation (Hassold et al., 2021; Hassold & Hunt, 2001; Koehler et al., 1996; Nagaoka et al., 2012; Nambiar et al., 2019; Ottolini et al., 2015). In contrast, in holocentric chromosomes, terminal chiasmata are common (de Bigliardo et al., 2011; Heckmann et al., 2014; John, 1990; Lukhtanov et al., 2018; Nokkala et al., 2004; White, 1973; Wrensch et al., 1994). Nonetheless, since terminal crossovers do not involve exchanges of genes, our characterization of the recombination landscape appears largely complete.

Heterochiasmy and sex-specific recombination landscape

The genetic map of the bulb mite reveals marked sex-based differences in recombination rates: females exhibit rates nearly double those of males. Bulb mites show fairly similar recombination landscapes in both sexes, with recombination rates increasing towards chromosome ends (Figure 2A). This finding diverges from those in the majority of taxa studied so far, where males generally show higher recombination rates at telomeres and females at chromosome centers, a difference often linked to meiotic driver defense mechanisms (Brandvain & Coop, 2012; Haig, 2010; Talbert, Bayes, et al., 2009). In contrast, the bulb mite's sex-specific genetic map demonstrates the absence of increased recombination in female chromosome centers. This finding supports the hypothesis that holocentricity mitigates centromere-biased meiotic drive. However, to generalize our findings, additional sex-specific genetic maps from other holocentric taxa are necessary.

Despite similar recombination landscapes (Figure 2A), females exhibit intrachromosomal shuffling rates that are three times higher than in males. This disparity between sexes therefore appears to be largely due to a higher overall frequency of crossovers in females, rather than differences in recombination landscape. This is supported by the observation that periphery bias does not significantly differ between males and females. The difference in crossover location between sexes may stem from sex-specific crossover interference, which more strongly affects male crossovers, increasing physical distance between subsequent recombination at the same chromosome (Falque et al., 2007; Haenel et al., 2018; Otto & Payseur, 2019; Zhang et al., 2014), or from the sex difference in meiosis progression during synapsis (Cahoon et al., 2023; Cahoon & Libuda, 2019; Zickler & Kleckner, 2016). This pattern, with male recombination restricted to distal parts of chromosomes, aligns with observations in fish and amphibians (Bergero et al., 2019; Brekke et al., 2023; Brelsford et al., 2016; Jeffries et al., 2018; Kai et al., 2011; Sardell et al., 2018).

Heterochiasmy, the difference in recombination rates between sexes, is proposed to evolve in the sex that experiences more intense selection to maintain beneficial allele combinations (Sardell & Kirkpatrick, 2020; Trivers, 1988). In bulb mite males, intense sexual selection involves sperm competition and physical contests, initiated by fighter males and sometimes escalating to lethality (Radwan, 1997; Radwan et al., 2000). Being an effective fighter requires co-expression of the weapon with behavioral and physiological traits (e.g. aggression, motor patterns and energy mobilization), which could be facilitated if alleles making good fighters, but poor scramblers are co-inherited. It is therefore suggestive that a large region on chromosome 7, where an important weapon-determining region has been located (Chmielewski et al., unpublished data; Parrett et al., 2022), coincides with a region with a markedly low male recombination rate, despite it being at the end of a chromosome (Figure 1A). On the other hand, it has been suggested that the sexual selection might promote increased recombination (Burt et al., 1991; Felsenstein, 1988; Smith, 1985), although empirical evidence does not support increased map length in the sex under stronger selection (Cooney et al.,

2021; Mank, 2009). An alternative explanation for heterochiasmy involves sexual antagonism. Sardell & Kirkpatrick (2020) proposed a model where conflict arises over the epistasis between alleles controlling the expression of a sexually antagonistic trait, with males benefitting from high linkage disequilibrium to maintain its high expression, while females gain from disrupting this allele association to mitigate fitness decrease associated with the pleiotropic effect of the male trait. This hypothesis has been supported in guppies (*Poecilia reticulata*), where strong heterochiasmy largely limits male recombination to a small, terminal pseudoautosomal region, whereas female recombination remains relatively uniform across the sex chromosome carrying sexually antagonistic color traits (Bergero et al., 2019; Charlesworth et al., 2020). Sexual antagonism may also shape heterochiasmy in bulb mites, the thick legs serving as a weapon are not expressed in females, but underlying genes appear to be associated with negative pleiotropic effects on female fitness (Joag et al., 2016; Łukasiewicz et al., 2020; Plesnar Bielak et al., 2014)

Genomic features correlated with local recombination rate

Recombination occurs mainly in open chromatin, gene-rich regions, resulting in positive correlations with gene density, epigenetic modifications, and GC content (Arndt et al., 2005; Brazier & Glémin, 2022; Haenel et al., 2018; Kyriacou et al., 2023; Peñalba & Wolf, 2020; Stapley et al., 2017; Thuriaux, 1977), while within dense heterochromatin crossover rate is reduced, permitting transposable elements to accumulate, potentially disrupting gene expression and structure. Deciphering causative factors in this covariation network is complex. Contrary to expectations, we demonstrated that the recombination rate positively correlates with the repeat density, but negatively with the gene density and the distance to chromosome ends, suggesting that crossovers mostly occur in gene-poor, repeat-rich areas near chromosome ends (Figure 4). Similarly, in holocentric organisms like *C. elegans* or some lepidopterans, where gene density drops at chromosome ends, no discernible correlation between recombination rate and the density of coding sequence was reported (Bernstein & Rockman, 2016; Stapley et al., 2017; Talla et al., 2019; Torres et al., 2023). This highlights that recombination patter may vary with chromosome types.

Surprisingly, we found no link between recombination rates and GC content in bulb mites, despite GC-biased gene conversion being a known driver of the correlation between recombination rates and GC content (Bolívar et al., 2019; Duret & Galtier, 2009; Mugal et al., 2015; Webster & Hurst, 2012). The absence of this association in bulb mites might be explained by the heterogeneous distribution of GC content across chromosomes, peaking in gene-dense central regions and similarly elevated in the highly recombining chromosome ends (Figure 3B). Yet, among holocentric organisms, the relationship between recombination rate and GC content shows variable patterns, ranging from negative association (Bernstein & Rockman, 2016; Kaur & Rockman, 2014; Torres et al., 2023) to positive ones (Stapley et al., 2017) suggesting a complex interplay between GC-biased gene conversion and opposing mutation bias toward AT nucleotides (Boman et al., 2021).

The positive correlation between recombination rate and the abundance of repetitive elements reflects the enrichment of repeats at the highly recombining chromosome ends (Figure 3C). Typically, regions with high recombination rate are thought to be more effective in purging transposable elements due to the effects mentioned above, and to decreased Hill-Robertson interference which enhances the effectiveness of purifying selection (Kent et al., 2017; Stapley et al., 2017). The prevalence of TEs in areas of high recombination may be attributed to their role in repairing double-strand breaks associated with recombination process (Onozawa et al., 2014), along with a propensity for certain TEs to integrate into distal parts of chromosomes (Kejnovsky et al., 2006; Pardue & DeBaryshe, 2011; Zou et al., 1996). For example, certain transposon types show a positive correlation with recombination rates in organisms such as *C. elegans* (Duret et al., 2000) and Lepidoptera

(Cicconardi et al., 2021; Stapley et al., 2017; Torres et al., 2023), as well as birds (Kawakami et al., 2014; Singhal et al., 2015).

In conclusion, our study presents the first sex-specific genetic linkage map for a gonochoristic organism with holocentric chromosomes, the bulb mite (*Rhizoglyphus robini*). Our comprehensive analysis shows that this species' recombination landscape is similar in males and females across most of the genome, supporting the hypothesis that the female recombination rate is shaped to counteract centromere-associated meiotic drive in species with monocentric chromosomes. Lower recombination rate in males may facilitate the maintenance of male-beneficial allele combinations by reducing the exchange of DNA between homologous chromosomes. This may be particularly pronounced in areas harboring genes under sexual selection, such as those located on chromosome 7 of the bulb mite. The bulb mite genome's structure and recombination patterns, including a high density of repeat elements at the chromosome ends and a concentration of genes in the central regions, illustrate the complex interplay between genomic architecture and recombination landscapes, and opens avenues for further research on the implications of holocentric chromosome structure for genome evolution.

Data availability

Raw sequence data have been deposited in NCBI Sequence Read Archive (BioProject PRJNA1088092). Code needed to repeat analyses has been deposited in GitHub (https://github.com/sebchm/genetic-map-of-the-bulb-mite) and datafiles are publicly available at Zenodo (DOI: 10.5281/zenodo.10959789). Additionally, GFF files with annotation of genes and repeat elements have been uploaded to ORCAE (https://bioinformatics.psb.ugent.be/orcae/overview/Rhrob).

Acknowlegements

We thank Aleksandra Łukasiewicz and Agnieszka Szubert-Kruszyńska for performing the crosses, Pasi Rastas for his generous advice on map construction and Deborah Charlesworth for her comments on the earlier version of the manuscript. Computations were partly performed at the Poznan Supercomputing and Networking Centre. This work was supported by National Science Centre grant no. 2017/27/B/NZ8/00077 awarded to J.R.

Literature Cited

Anderson, N., Jaron, K. S., Hodson, C. N., Couger, M. B., Sevcık, J., Weinstein, B., Pirro, S., Ross, L., & Roy, S. W. (2022). Gene-rich X chromosomes implicate intragenomic conflict in the evolution of bizarre genetic systems. *Proceedings of the National Academy of Sciences of the United States of America*, *119*(23), 1–7. https://doi.org/10.1073/pnas.2122580119

Arndt, P. F., Hwa, T., & Petrov, D. A. (2005). Substantial regional variation in substitution rates in the human genome: Importance of GC content, gene density, and telomere-specific effects. *Journal of Molecular Evolution*, *60*(6), 748–763. https://doi.org/10.1007/s00239-004-0222-5

Berdan, E. L., Blanckaert, A., Butlin, R. K., & Bank, C. (2021). Deleterious mutation accumulation and the long-term fate of chromosomal inversions. *PLOS Genetics*, *17*(3), e1009411. https://doi.org/10.1371/journal.pgen.1009411

Bergero, R., Gardner, J., Bader, B., Yong, L., & Charlesworth, D. (2019). Exaggerated heterochiasmy in a fish with sex-linked male coloration polymorphisms. *Proceedings of the National Academy of Sciences of the United States of America*, *116*(14), 6924–6931. https://doi.org/10.1073/pnas.1818486116

Bernstein, M. R., & Rockman, M. V. (2016). Fine-Scale Crossover Rate Variation on the *Caenorhabditis elegans* X Chromosome. *G3 Genes|Genomes|Genetics*, *6*(6), 1767–1776. https://doi.org/10.1534/g3.116.028001

Bolger, A. M., Lohse, M., & Usadel, B. (2014). Trimmomatic: A flexible trimmer for Illumina sequence data. *Bioinformatics*, *30*(15), 2114–2120. https://doi.org/10.1093/bioinformatics/btu170

Bolívar, P., Guéguen, L., Duret, L., Ellegren, H., & Mugal, C. F. (2019). GC-biased gene conversion conceals the prediction of the nearly neutral theory in avian genomes 06 Biological Sciences 0604 Genetics. *Genome Biology*, *20*(1), 1–13. https://doi.org/10.1186/s13059-018-1613-z

Boman, J., Mugal, C. F., & Backström, N. (2021). The Effects of GC-Biased Gene Conversion on Patterns of Genetic Diversity among and across Butterfly Genomes. *Genome Biology and Evolution*, *13*(5), 1–19. https://doi.org/10.1093/gbe/evab064

Brandvain, Y., & Coop, G. (2012). Scrambling eggs: Meiotic drive and the evolution of female recombination rates. *Genetics*, *190*(2), 709–723. https://doi.org/10.1534/genetics.111.136721

Brazier, T., & Glémin, S. (2022). Diversity and determinants of recombination landscapes in flowering plants. *PLoS Genetics*, *18*(8), 1–29. https://doi.org/10.1371/journal.pgen.1010141

Brekke, C., Johnston, S. E., Knutsen, T. M., & Berg, P. (2023). Genetic architecture of individual meiotic crossover rate and distribution in Atlantic Salmon. *Scientific Reports*, *13*(1), 20481. https://doi.org/10.1038/s41598-023-47208-3

Brelsford, A., Rodrigues, N., & Perrin, N. (2016). High-density linkage maps fail to detect any genetic component to sex determination in a *Rana temporaria* family. *Journal of Evolutionary Biology*, *29*(1), 220–225. https://doi.org/10.1111/jeb.12747

Burt, A., Bell, G., & Harvey, P. H. (1991). Sex differences in recombination. *Journal of Evolutionary Biology*, *4*(2), 259–277. https://doi.org/10.1046/j.1420-9101.1991.4020259.x

Cahoon, C. K., & Libuda, D. E. (2019). Leagues of their own: sexually dimorphic features of meiotic prophase I. *Chromosoma*, *128*(3), 199–214. https://doi.org/10.1007/s00412-019-00692-x

Cahoon, C. K., Richter, C. M., Dayton, A. E., & Libuda, D. E. (2023). Sexual dimorphic regulation of recombination by the synaptonemal complex in *C. elegans*. *ELife*, *12*. https://doi.org/10.7554/eLife.84538

Charlesworth, D. (2017). Evolution of recombination rates between sex chromosomes. *Philosophical Transactions of the Royal Society B: Biological Sciences*, *372*(1736). https://doi.org/10.1098/rstb.2016.0456

Charlesworth, D., Bergero, R., Graham, C., Gardner, J., & Yong, L. (2020). Locating the sex determining region of linkage group 12 of guppy (*Poecilia reticulata*). *G3: Genes, Genomes, Genetics*, *10*(10), 3639–3649. https://doi.org/10.1534/g3.120.401573

Cicconardi, F., Lewis, J. J., Martin, S. H., Reed, R. D., Danko, C. G., & Montgomery, S. H. (2021). Chromosome Fusion Affects Genetic Diversity and Evolutionary Turnover of Functional Loci but Consistently Depends on Chromosome Size. *Molecular Biology and Evolution*, *38*(10), 4449–4462. https://doi.org/10.1093/molbev/msab185

Clark, F. E., & Akera, T. (2021). Unravelling the mystery of female meiotic drive: where we are. *Open Biology*, *11*(9). https://doi.org/10.1098/rsob.210074

Connallon, T., & Clark, A. G. (2010). Sex linkage, sex-specific selection, and the role of recombination in the evolution of sexually dimorphic gene expression. *Evolution*, *64*(12), 3417–3442. https://doi.org/10.1111/j.1558-5646.2010.01136.x

Cooney, C. R., Mank, J. E., & Wright, A. E. (2021). Constraint and divergence in the evolution of male and female recombination rates in fishes. *Evolution*, *75*(11), 2857–2866. https://doi.org/10.1111/evo.14357

Coop, G., & Przeworski, M. (2007). An evolutionary view of human recombination. *Nature Reviews Genetics*, *8*(1), 23–34. https://doi.org/10.1038/nrg1947

de Bigliardo, G. R., Virla, E. G., Caro, S., & Dasso, S. M. (2011). Karyotype and male pre-reductional meiosis of the sharpshooter *Tapajosa rubromarginata* (Hemiptera: Cicadellidae). *Revista de Biologia Tropical*, *59*(1), 309–314. https://doi.org/10.15517/rbt.v59i1.3200

Talbert, P. B., Bayes, J. J., & Henikoff, S. (2009). Evolution of Centromeres and Kinetochores: A Two-Part Fugue. In *The Kinetochore:* (pp. 1–37). Springer New York. https://doi.org/10.1007/978-0-387-69076-6_7

Díaz, A., Okabe, K., Eckenrode, C. (2002). Biology, ecology, and management of the bulb mites of the genus *Rhizoglyphus* (Acari: Acaridae). *Entomologia Experimentalis et Applicata*, *103*(3), 239–248. https://doi.org/https://doi.org/10.1023/A:1006304300657

Duret, L., & Galtier, N. (2009). Biased gene conversion and the evolution of mammalian genomic landscapes. *Annual Review of Genomics and Human Genetics*, *10*, 285–311. https://doi.org/10.1146/annurev-genom-082908-150001

Duret, L., Marais, G., & Biemont, C. (2000). Transposons but not retrotransposons are located preferentially in regions of high recombination rate in *Caenorhabditis elegans*. *Genetics*, *156*(4), 1661–1669. https://doi.org/10.1093/genetics/156.4.1661

Ellegren, H., & Galtier, N. (2016). Determinants of genetic diversity. *Nature Reviews Genetics*, *17*(7), 422–433. https://doi.org/10.1038/nrg.2016.58

Falque, M., Mercier, R., Mézard, C., De Vienne, D., & Martin, O. C. (2007). Patterns of recombination and MLH1 foci density along mouse chromosomes: Modeling effects of interference and obligate chiasma. *Genetics*, *176*(3), 1453–1467. https://doi.org/10.1534/genetics.106.070235

Felsenstein, J. (1988). Sex and the evolution of recombination. In Richard E. Michod; Bruce R. Levin (Ed.), *The Evolution of sex: an examination of current ideas* (pp. 74–86). Sinauer Associates Inc.

Fierst, J. L. (2015). Using linkage maps to correct and scaffold de novo genome assemblies: methods, challenges, and computational tools. *Frontiers in Genetics*, *6*, 1–8. https://doi.org/10.3389/fgene.2015.00220

Flynn, J. M., Hubley, R., Goubert, C., Rosen, J., Clark, A. G., Feschotte, C., & Smit, A. F. (2020). RepeatModeler2 for automated genomic discovery of transposable element families. *Proceedings of the National Academy of Sciences of the United States of America*, *117*(17), 9451–9457. https://doi.org/10.1073/pnas.1921046117

Gerson, U., Cohen, E., & Capua, S. (1991). Bulb mite, *Rhizoglyphus robini* (Astigmata: Acaridae) as an experimental animal. *Experimental & Applied Acarology*, *12*(1–2), 103–110. https://doi.org/10.1007/BF01204403

Gregory, T. R., & Young, M. R. (2020). Small genomes in most mites (but not ticks). *International Journal of Acarology*, *46*(1), 1–8. https://doi.org/10.1080/01647954.2019.1684561

Haenel, Q., Laurentino, T. G., Roesti, M., & Berner, D. (2018). Meta-analysis of chromosome-scale crossover rate variation in eukaryotes and its significance to evolutionary genomics. *Molecular Ecology*, *27*(11), 2477–2497. https://doi.org/10.1111/mec.14699

Haig, D. (2010). Games in tetrads: Segregation, recombination, and meiotic drive. *American Naturalist*, *176*(4), 404–413. https://doi.org/10.1086/656265

Hassold, T., & Hunt, P. (2001). To err (meiotically) is human: The genesis of human aneuploidy. *Nature Reviews Genetics*, *2*(4), 280–291. https://doi.org/10.1038/35066065

Hassold, T., Maylor-Hagen, H., Wood, A., Gruhn, J., Hoffmann, E., Broman, K. W., & Hunt, P. (2021). Failure to recombine is a common feature of human oogenesis. *American Journal of Human Genetics*, *108*(1), 16–24. https://doi.org/10.1016/j.ajhg.2020.11.010

Heckmann, S., Jankowska, M., Schubert, V., Kumke, K., Ma, W., & Houben, A. (2014). Alternative meiotic chromatid segregation in the holocentric plant *Luzula elegans*. *Nature Communications*, *5*, 1–10. https://doi.org/10.1038/ncomms5979

Huang, S., Kang, M., & Xu, A. (2017). HaploMerger2: Rebuilding both haploid sub-assemblies from high-heterozygosity diploid genome assembly. *Bioinformatics*, *33*(16), 2577–2579. https://doi.org/10.1093/bioinformatics/btx220

Hughes, S. E., & Hawley, R. S. (2020). Meiosis: Location, Location, Location, How Crossovers Ensure Segregation. *Current Biology*, *30*(7), R311–R313. https://doi.org/10.1016/j.cub.2020.02.020

Hunt, P. A., & Hassold, T. J. (2002). Sex matters in meiosis. *Science*, *296*(5576), 2181–2183. https://doi.org/10.1126/science.1071907

Jeffries, D. L., Lavanchy, G., Sermier, R., Sredl, M. J., Miura, I., Borzée, A., Barrow, L. N., Canestrelli, D., Crochet, P. A., Dufresnes, C., Fu, J., Ma, W. J., Garcia, C. M., Ghali, K., Nicieza, A. G., O'Donnell, R. P., Rodrigues, N., Romano, A., Martínez-Solano, Í., … Perrin, N. (2018). A rapid rate of sex-chromosome turnover and non-random transitions in true frogs. *Nature Communications*, *9*(1). https://doi.org/10.1038/s41467-018-06517-2

Joag, R., Stuglik, M., Konczal, M., Plesnar-Bielak, A., Skrzynecka, A., Babik, W., & Radwan, J. (2016). Transcriptomics of intralocus sexual conflict: Gene expression patterns in females change in response to selection on a male secondary sexual trait in the bulb mite. *Genome Biology and Evolution*, *8*(8), 2351–2357. https://doi.org/10.1093/gbe/evw169

John, B. (1990). *Meiosis*. Cambridge University Press.

Jurka, J., Kapitonov, V. V., Pavlicek, A., Klonowski, P., Kohany, O., & Walichiewicz, J. (2005). Repbase Update, a database of eukaryotic repetitive elements. *Cytogenetic and Genome Research*, *110*(1–4), 462–467. https://doi.org/10.1159/000084979

Kai, W., Kikuchi, K., Tohari, S., Chew, A. K., Tay, A., Fujiwara, A., Hosoya, S., Suetake, H., Naruse, K., Brenner, S., Suzuki, Y., & Venkatesh, B. (2011). Integration of the genetic map and genome assembly of fugu facilitates insights into distinct features of genome evolution in teleosts and mammals. *Genome Biology and Evolution*, *3*(1), 424–442. https://doi.org/10.1093/gbe/evr041

Kasimatis, K. R., Sánchez-Ramírez, S., & Stevenson, Z. C. (2021). Sexual Dimorphism through the Lens of Genome Manipulation, Forward Genetics, and Spatiotemporal Sequencing. *Genome Biology and Evolution*, *13*(2), 1–13. https://doi.org/10.1093/gbe/evaa243

Kaur, T., & Rockman, M. V. (2014). Crossover heterogeneity in the absence of hotspots in *Caenorhabditis elegans*. *Genetics*, *196*(1), 137–148. https://doi.org/10.1534/genetics.113.158857

Kawakami, T., Smeds, L., Backström, N., Husby, A., Qvarnström, A., Mugal, C. F., Olason, P., & Ellegren, H. (2014). A high-density linkage map enables a second-generation collared flycatcher genome assembly and reveals the patterns of avian recombination rate variation and chromosomal evolution. *Molecular Ecology*, *23*(16), 4035–4058. https://doi.org/10.1111/mec.12810

Kejnovsky, E., Kubat, Z., Macas, J., Hobza, R., Mracek, J., & Vyskot, B. (2006). Retand: a novel family of gypsy-like retrotransposons harboring an amplified tandem repeat. *Molecular Genetics and Genomics*, *276*(3), 254–263. https://doi.org/10.1007/s00438-006-0140-x

Kent, T. V., Uzunović, J., & Wright, S. I. (2017). Coevolution between transposable elements and recombination. *Philosophical Transactions of the Royal Society B: Biological Sciences*, *372*(1736). https://doi.org/10.1098/rstb.2016.0458

Koehler, K. E., Hawley, R. S., Sherman, S., & Hassold, T. (1996). Recombination and nondisjunction in humans and flies. *Human Molecular Genetics*, *5*(REVIEW), 1495–1504. https://doi.org/10.1093/hmg/5.supplement_1.1495

Král, J., Forman, M., Kořínková, T., Lerma, A. C. R., Haddad, C. R., Musilová, J., Řezáč, M., Herrera, I. M. Á., Thakur, S., Dippenaar-Schoeman, A. S., Marec, F., Horová, L., & Bureš, P. (2019). Insights into the karyotype and genome evolution of haplogyne spiders indicate a polyploid origin of lineage with holokinetic chromosomes. *Scientific Reports*, *9*(1), 1–14. https://doi.org/10.1038/s41598-019-39034-3

Kyriacou, R. G., Mulhair, P. O., & Holland, P. W. H. (2023). GC content across insect genomes: phylogenetic patterns, causes and consequences. *BioRxiv*, 2023.09.11 [accessed 2024 April 5th]. https://www.biorxiv.org/content/10.1101/2023.09.11.557135v1

Lenormand, T. (2003). The evolution of sex dimorphism in recombination. *Genetics*, *163*(2), 811–822. https://doi.org/10.1093/genetics/163.2.811

Lenormand, T., & Dutheil, J. (2005). *Recombination Difference between Sexes: A Role for Haploid Selection*. *3*(3). https://doi.org/10.1371/journal.pbio.0030063

Li, H. (2013). *Aligning sequence reads, clone sequences and assembly contigs with BWA-MEM*. *00*(00), 1–3. http://arxiv.org/abs/1303.3997

Li, H. (2018). Minimap2: Pairwise alignment for nucleotide sequences. *Bioinformatics*, *34*(18), 3094–3100. https://doi.org/10.1093/bioinformatics/bty191

Li, H., Handsaker, B., Wysoker, A., Fennell, T., Ruan, J., Homer, N., Marth, G., Abecasis, G., & Durbin, R. (2009). The Sequence Alignment/Map format and SAMtools. *Bioinformatics*, *25*(16), 2078–2079. https://doi.org/10.1093/bioinformatics/btp352

Li, Y., Park, H., Smith, T. E., Moran, N. A., & Singh, N. (2019). Gene Family Evolution in the Pea Aphid Based on Chromosome-Level Genome Assembly. *Molecular Biology and Evolution*, *36*(10), 2143–2156. https://doi.org/10.1093/molbev/msz138

Liu, H., Jiang, F., Wang, S., Wang, H., Wang, A., Zhao, H., Xu, D., Yang, B., & Fan, W. (2022). Chromosome-level genome of the globe skimmer dragonfly (*Pantala flavescens*). *GigaScience*, *11*, 1–8. https://doi.org/10.1093/gigascience/giac009

Łukasiewicz, A., Niśkiewicz, M., & Radwan, J. (2020). Sexually selected male weapon is associated with lower inbreeding load but higher sex load in the bulb mite. *Evolution*, *74*(8), 1851–1855. https://doi.org/10.1111/evo.14033

Lukhtanov, V. A., Dinca, V., Friberg, M., Síchová, J., Olofsson, M., Vila, R., Marec, F., & Wiklund, C. (2018). Versatility of multivalent orientation, inverted meiosis, and rescued fitness in holocentric chromosomal hybrids. *Proceedings of the National Academy of Sciences of the United States of America*, *115*(41), E9610–E9619. https://doi.org/10.1073/pnas.1802610115

Mank, J. E. (2009). The evolution of heterochiasmy: the role of sexual selection and sperm competition in determining sex-specific recombination rates in eutherian mammals. *Genetics Research*, *91*(5), 355–363. https://doi.org/10.1017/S0016672309990255

Meneely, P. M., Farago, A. F., & Kauffman, T. M. (2002). Crossover distribution and high interference for both the X chromosome and an autosome during oogenesis and spermatogenesis in *Caenorhabditis elegans*. *Genetics*, *162*(3), 1169–1177. https://doi.org/10.1093/genetics/162.3.1169

Mugal, C. F., Weber, C. C., & Ellegren, H. (2015). GC-biased gene conversion links the recombination landscape and demography to genomic base composition: GC-biased gene conversion drives genomic base composition across a wide range of species. *BioEssays*, *37*(12), 1317–1326. https://doi.org/10.1002/bies.201500058

Nagaoka, S. I., Hassold, T. J., & Hunt, P. A. (2012). Human aneuploidy: mechanisms and new insights into an age-old problem. *Nature Reviews Genetics*, *13*(7), 493–504. https://doi.org/10.1038/nrg3245

Nambiar, M., Chuang, Y.-C., & Smith, G. R. (2019). Distributing meiotic crossovers for optimal fertility and evolution. *DNA Repair*, *81*, 102648. https://doi.org/10.1016/j.dnarep.2019.102648

Nambiar, M., & Smith, G. R. (2016). Repression of harmful meiotic recombination in centromeric regions. *Seminars in Cell and Developmental Biology*, *54*, 188–197. https://doi.org/10.1016/j.semcdb.2016.01.042

Näsvall, K., Boman, J., Höök, L., Vila, R., Wiklund, C., & Backström, N. (2023). Nascent evolution of recombination rate differences as a consequence of chromosomal rearrangements. *PLoS Genetics*, *19*(8), 1–21. https://doi.org/10.1371/journal.pgen.1010717

Nokkala, S., Kuznetsova, V. G., Maryanska-Nadachowska, A., & Nokkala, C. (2004). Holocentric chromosomes in meiosis. I. Restriction of the number of chiasmata in bivalents. *Chromosome Research*, *12*(7), 733–739. https://doi.org/10.1023/B:CHRO.0000045797.74375.70

Onozawa, M., Zhang, Z., Kim, Y. J., Goldberg, L., Varga, T., Bergsagel, P. L., Kuehl, W. M., & Aplan, P. D. (2014). Repair of DNA double-strand breaks by templated nucleotide sequence insertions derived from distant regions of the genome. *Proceedings of the National Academy of Sciences of the United States of America*, *111*(21), 7729–7734. https://doi.org/10.1073/pnas.1321889111

Otto, S. P., & Payseur, B. A. (2019). Crossover Interference: Shedding Light on the Evolution of Recombination. *Annual Review of Genetics*, *53*, 19–44. https://doi.org/10.1146/annurev-genet-040119-093957

Ottolini, C. S., Newnham, L. J., Capalbo, A., Natesan, S. A., Joshi, H. A., Cimadomo, D., Griffin, D. K., Sage, K., Summers, M. C., Thornhill, A. R., Housworth, E., Herbert, A. D., Rienzi, L., Ubaldi, F. M., Handyside, A. H., & Hoffmann, E. R. (2015). Genome-wide maps of recombination and chromosome segregation in human oocytes and embryos show selection for maternal recombination rates. *Nature Genetics*, *47*(7), 727–735. https://doi.org/10.1038/ng.3306

Pardue, M. Lou, & DeBaryshe, P. G. (2011). Retrotransposons that maintain chromosome ends. *Proceedings of the National Academy of Sciences of the United States of America*, *108*(51), 20317–20324. https://doi.org/10.1073/pnas.1100278108

Parrett, J. M., Chmielewski, S., Aydogdu, E., Łukasiewicz, A., Rombauts, S., Szubert-Kruszyńska, A., Babik, W., Konczal, M., & Radwan, J. (2022). Genomic evidence that a sexually selected trait captures genome-wide variation and facilitates the purging of genetic load. *Nature Ecology & Evolution*, *6*(9), 1330–1342. https://doi.org/10.1038/s41559-022-01816-w

Parrett, J. M., Łukasiewicz, A., Chmielewski, S., Szubert-Kruszyńska, A., Maurizio, P. L., Grieshop, K., & Radwan, J. (2023). A sexually selected male weapon characterized by strong additive genetic variance and no evidence for sexually antagonistic polyphenic maintenance. *Evolution*, *77*(6), 1289–1302. https://doi.org/10.1093/evolut/qpad039

Peñalba, J. V., & Wolf, J. B. W. (2020). From molecules to populations: appreciating and estimating recombination rate variation. *Nature Reviews Genetics*, *21*(8), 476–492. https://doi.org/10.1038/s41576-020-0240-1

Peterson, A. L., & Payseur, B. A. (2021). Sex-specific variation in the genome-wide recombination rate. *Genetics*, *217*(1), 1–11. https://doi.org/10.1093/GENETICS/IYAA019

Plesnar Bielak, A., Skrzynecka, A. M., Miler, K., & Radwan, J. (2014). Selection for alternative male reproductive tactics alters intralocus sexual conflict. *Evolution*, *68*(7), 2137–2144. https://doi.org/10.1111/evo.12409

Plesnar-Bielak, A., Jawor, A., & Kramarz, P. E. (2013). Complex response in size-related traits of bulb mites (*Rhizoglyphus robini*) under elevated thermal conditions-An experimental evolution approach. *Journal of Experimental Biology*, *216*(24), 4542–4548. https://doi.org/10.1242/jeb.090951

Plesnar-Bielak, A., Parrett, J. M., Chmielewski, S., Dudek, K., Łukasiewicz, A., Marszałek, M., Babik, W., & Konczal, M. (2022). Transcriptomics of differences in thermal plasticity associated with selection for an exaggerated male sexual trait. *ResearchSquare*, preprint [accessed 2024 April 5th]. https://doi.org/https://doi.org/10.21203/rs.3.rs-1862013/v1

Quinlan, A. R., & Hall, I. M. (2010). BEDTools: A flexible suite of utilities for comparing genomic features. *Bioinformatics*, *26*(6), 841–842. https://doi.org/10.1093/bioinformatics/btq033

Radwan, J. (1997). Sperm precedence in the bulb mite, *Rhizoglyphus robini*: Context-dependent variation. *Ethology Ecology and Evolution*, *9*(4), 373–383. https://doi.org/10.1080/08927014.1997.9522879

Radwan, J. (2007). Sexual selection and conflict in the bulb mite, *Rhizoglyphus robini* (Astigmata: Acaridae). *Experimental and Applied Acarology*, *42*(3), 151–158. https://doi.org/10.1007/s10493-007-9086-x

Radwan, J. (2009). Alternative Mating Tactics in Acarid Mites. In *Advances in the Study of Behavior* (1st ed., Vol. 39, Issue 09, pp. 185–208). Elsevier Inc. https://doi.org/10.1016/S0065-3454(09)39006-3

Radwan, J., Czyz, M., Konior, M., & Kołodziejczyk, M. (2000). Aggressiveness in two male morphs of the bulb mite *Rhizoglyphus robini*. *Ethology*, *106*(1), 53–62. https://doi.org/10.1046/j.1439-0310.2000.00498.x

Rastas, P. (2017). Lep-MAP3: Robust linkage mapping even for low-coverage whole genome sequencing data. *Bioinformatics*, *33*(23), 3726–3732. https://doi.org/10.1093/bioinformatics/btx494

Rastas, P. (2020). Lep-Anchor: Automated construction of linkage map anchored haploid genomes. *Bioinformatics*, *36*(8), 2359–2364. https://doi.org/10.1093/bioinformatics/btz978

Ritz, K. R., Noor, M. A. F., & Singh, N. D. (2017). Variation in Recombination Rate: Adaptive or Not? *Trends in Genetics*, *33*(5), 364–374. https://doi.org/10.1016/j.tig.2017.03.003

Sardell, J. M., Cheng, C., Dagilis, A. J., Ishikawa, A., Kitano, J., Peichel, C. L., & Kirkpatrick, M. (2018). Sex differences in recombination in sticklebacks. *G3: Genes, Genomes, Genetics*, *8*(6), 1971–1983. https://doi.org/10.1534/g3.118.200166

Sardell, J. M., & Kirkpatrick, M. (2020). Sex differences in the recombination landscape. *American Naturalist*, *195*(2), 361–379. https://doi.org/10.1086/704943

Stapley, J., Feulner, P. G. D., Johnston, S. E., Santure, A. W., & Smadja, C. M. (2017). Variation in recombination frequency and distribution across eukaryotes: patterns and processes. *Philosophical Transactions of the Royal Society B: Biological Sciences*, *372*(1736), 20160455. https://doi.org/10.1098/rstb.2016.0455

Singhal, S., Leffler, E. M., Sannareddy, K., Turner, I., Venn, O., Hooper, D. M., Strand, A. I., Li, Q., Raney, B., Balakrishnan, C. N., Griffith, S. C., McVean, G., & Przeworski, M. (2015). Stable recombination hotspots in birds. *Science*, *350*(6263), 928–932. https://doi.org/10.1126/science.aad0843

Smallegange, I. M., Caswell, H., Toorians, M. E. M., & de Roos, A. M. (2017). Mechanistic description of population dynamics using dynamic energy budget theory incorporated into integral projection models. *Methods in Ecology and Evolution*, *8*(2), 146–154. https://doi.org/10.1111/2041-210X.12675

Smith, J. M. (1985). The evolution of recombination. *Journal of Genetics*, *64*(2–3), 159–171. https://doi.org/10.1007/BF02931144

Stapley, J., Feulner, P. G. D., Johnston, S. E., Santure, A. W., & Smadja, C. M. (2017). Variation in recombination frequency and distribution across eukaryotes: Patterns and processes. *Philosophical Transactions of the Royal Society B: Biological Sciences*, *372*(1736). https://doi.org/10.1098/rstb.2016.0455

Sterck, L., Billiau, K., Abeel, T., Rouzé, P., & Van De Peer, Y. (2012). ORCAE: Online resource for community annotation of eukaryotes. *Nature Methods*, *9*(11), 1041. https://doi.org/10.1038/nmeth.2242

Sugimoto, N., Takahashi, A., Ihara, R., Itoh, Y., Jouraku, A., Van Leeuwen, T., & Osakabe, M. (2020). QTL mapping using microsatellite linkage reveals target-site mutations associated with high levels of resistance against three mitochondrial complex II inhibitors in *Tetranychus urticae*. *Insect Biochemistry and Molecular Biology*, *123*(February), 103410. https://doi.org/10.1016/j.ibmb.2020.103410

Sullivan, G. T., & Ozman-Sullivan, S. K. (2021). Alarming evidence of widespread mite extinctions in the shadows of plant, insect and vertebrate extinctions. *Austral Ecology*, *46*(1), 163–176. https://doi.org/10.1111/aec.12932

Talla, V., Soler, L., Kawakami, T., DincCrossed D Signf, V., Vila, R., Friberg, M., Wiklund, C., Backström, N., & Gonzalez, J. (2019). Dissecting the Effects of Selection and Mutation on Genetic Diversity in Three Wood White (*Leptidea*) Butterfly Species. *Genome Biology and Evolution*, *11*(10), 2875–2886. https://doi.org/10.1093/gbe/evz212

Tarailo-Graovac, M., & Chen, N. (2009). Using RepeatMasker to identify repetitive elements in genomic sequences. *Current Protocols in Bioinformatics*, *SUPPL. 25*, 1–14. https://doi.org/10.1002/0471250953.bi0410s25

The C. elegans Sequencing Consortium. (1998). Genome Sequence of the Nematode *C. elegans*: A Platform for Investigating Biology. *Science*, *282*(5396), 2012–2018. https://doi.org/10.1126/science.282.5396.2012

Thuriaux, P. (1977). Is recombination confined to structural genes on the eukaryotic genome? *Nature*, *268*(5619), 460–462. https://doi.org/10.1038/268460a0

Torres, A. P., Höök, L., Näsvall, K., Shipilina, D., Wiklund, C., Vila, R., Pruisscher, P., & Backström, N. (2023). The fine-scale recombination rate variation and associations with genomic features in a butterfly. *Genome Research*, *33*(5), 810–823. https://doi.org/10.1101/gr.277414.122

Trivers, R. (1988). The Evolution of Sex: An Examination of Current Ideas. In Richard E. Michod (Ed.), *The evolution of sex* (pp. 270–286). Sinauer Associates Inc.

Ullmann, A. J., Piesman, J., Dolan, M. C., & Black IV, W. C. (2003). A preliminary linkage map of the hard tick, *Ixodes scapularis*. *Insect Molecular Biology*, *12*(2), 201–210. https://doi.org/10.1046/j.1365-2583.2003.00402.x

Veller, C., Kleckner, N., & Nowak, M. A. (2019). A rigorous measure of genome-wide genetic shuffling that takes into account crossover positions and Mendel's second law. *Proceedings of the National Academy of Sciences of the United States of America*, *116*(5), 1659–1668. https://doi.org/10.1073/pnas.1817482116

Walter, D. E., & Proctor, H. C. (2013). Mites: Ecology, Evolution & Behaviour. In *Mites: Ecology, Evolution & Behaviour*. Springer Netherlands. https://doi.org/10.1007/978-94-007-7164-2

Webster, M. T., & Hurst, L. D. (2012). Direct and indirect consequences of meiotic recombination: Implications for genome evolution. *Trends in Genetics*, *28*(3), 101–109. https://doi.org/10.1016/j.tig.2011.11.002

Wellenreuther, M., & Bernatchez, L. (2018). Eco-Evolutionary Genomics of Chromosomal Inversions. *Trends in Ecology and Evolution*, *33*(6), 427–440. https://doi.org/10.1016/j.tree.2018.04.002

White, M. J. D. (1973). *Animal cytology and evolution* (3rd ed.). Cambridge University Press.

Wickham, H. (2016). *Elegant Graphics for Data Analysis*. Springer International Publishing. https://doi.org/10.1007/978-3-319-24277-4

Wilfert, L., Gadau, J., & Schmid-Hempel, P. (2007). Variation in genomic recombination rates among animal taxa and the case of social insects. *Heredity*, *98*(4), 189–197. https://doi.org/10.1038/sj.hdy.6800950

Wrensch, D. L., Kethley, J. B., & Norton, R. A. (1994). Cytogenetics of Holokinetic Chromosomes and Inverted Meiosis: Keys to the Evolutionary Success of Mites, with Generalizations on Eukaryotes. *Mites*, 282–343. https://doi.org/10.1007/978-1-4615-2389-5_11

Xiong, Q., Wan, A. T. Y., & Tsui, S. K.-W. (2020). A Mini-review of the Genomes and Allergens of Mites and Ticks. *Current Protein & Peptide Science*, *21*(2), 114–123. https://doi.org/10.2174/1389203720666190719150432

Zhang, L., Liang, Z., Hutchinson, J., & Kleckner, N. (2014). Crossover Patterning by the Beam-Film Model: Analysis and Implications. *PLoS Genetics*, *10*(1), e1004042. https://doi.org/10.1371/journal.pgen.1004042

Zhou, Y., Klimov, P. B., Gu, X., Yu, Z., Cui, X., Li, Q., Pan, R., Yuan, C., Cai, F., & Cui, Y. (2023). Chromosome-level genomic assembly and allergome inference reveal novel allergens in *Tyrophagus putrescentiae*. *Allergy: European Journal of Allergy and Clinical Immunology*, *78*(6), 1691–1695. https://doi.org/10.1111/all.15656

Zickler, D., & Kleckner, N. (2016). A few of our favorite things: Pairing, the bouquet, crossover interference and evolution of meiosis. *Seminars in Cell and Developmental Biology*, *54*, 135–148. https://doi.org/10.1016/j.semcdb.2016.02.024

Zou, S., Kim, J. M., & Voytas, D. F. (1996). The *Saccharomyces* retrotransposon Ty5 influences the organization of chromosome ends. *Nucleic Acids Research*, *24*(23), 4825–4831. https://doi.org/10.1093/nar/24.23.4825

Table 1. Overview of the experimental crosses and their reproductive output.

Family	dam line	sire line	F1 male morph	number of F2 individuals
A	scrambler-selected IN1	fighter-selected IW9	scrambler	32
B	scrambler-selected IN5	fighter-selected IW22	scrambler	32
C	fighter-selected IW15	scrambler-selected IN7	scrambler	60
D	scrambler-selected IN3	fighter-selected IW17	scrambler	59

Table 2. Summary of the linkage map for each chromosome and sex.

chromosome	physical length [Mb]	Genetic length [cM]		number of markers		F:M length ratio	recombination rate [cM/Mb]		periphery bias	
		female map	male map	female map	male map		female map	male map	female map	male map
1	50	46.3	7.2	9,616	9,616	6.43	0.93	0.14	2.95	3.46
2	33.8	27.7	17.4	32,822	32,821	1.59	0.82	0.51	3.69	2.92
3	33.3	40.9	23.9	57,804	57,804	1.71	1.23	0.72	3.64	2.91
4	32.5	37.4	19.1	66,884	66,884	1.96	1.15	0.59	2.92	3.11
5	31.3	41.4	25.7	1,988	1,986	1.61	1.32	0.82	2.99	2.22
6 (sex)	29.7	51.6	-	45,551	-	-	1.74	-	1.6	-
7	28.6	28.7	8.96	59,844	59,845	3.2	1	0.31	2.02	3.76
8	26.4	35.3	21.7	25,268	25,267	1.63	1.34	0.82	2.95	1.22
sum	**265.84**	**309.4**	**123.98**	**299,777**	**254,223**					

Table 3. Summary of repetitive elements annotated to the major repeat classes.

Repeat class	Type	Number of elements	Length occupied [bp]	Fraction of the genome
Interspersed elements	Unclassified	129,314	60,378,963	20.42%
	LTR elements	11,990	6,123,192	2.07%
	LINEs	6,672	4,141,649	1.40%
	DNA transposons	10,350	4,315,236	1.46%
	SINEs	0	0	0.00%
Simple repeats		106,850	5,864,289	1.98%
Satellites		4,634	1,279,523	0.43%
Small RNA		1,000	386,370	0.13%
Low complexity		16,073	798,431	0.27%